

Cite this: *RSC Adv.*, 2017, 7, 26559

# Sensing of hydrogen peroxide and glucose in human serum *via* quenching fluorescence of biomolecule-stabilized Au nanoclusters assisted by the Fenton reaction†

Chenghua Zong,<sup>a</sup> Min Wang,<sup>a</sup> Bo Li,<sup>a</sup> Xiaojun Liu,<sup>a</sup> Wenfeng Zhao,<sup>a</sup> Qingquan Zhang,<sup>a</sup> Aiye Liang<sup>b</sup> and Yang Yu<sup>id</sup>\*<sup>a</sup>

$\text{Fe}^{2+}$  can act as a catalyst to disproportionate hydrogen peroxide ( $\text{H}_2\text{O}_2$ ) to produce extremely reactive hydroxyl radicals ( $\cdot\text{OH}$ ) through the so-called Fenton reaction. Combining this reaction with the prominent sensitive nature of gold nanoclusters (Au NCs), we present herein a simple strategy of sensitive and rapid detection of  $\text{H}_2\text{O}_2$ . Compared with  $\text{H}_2\text{O}_2$ , the produced hydroxyl radical exhibits a much stronger oxidizing ability, and therefore could lead to a more efficient oxidation of the Au NCs and an improved sensitivity and oxidation rate. The results indicate that the detection limit for the determination of  $\text{H}_2\text{O}_2$  was  $0.2\ \mu\text{M}$  (signal/noise = 3) and the linear range was  $0.4\text{--}12\ \mu\text{M}$ . Furthermore, in combination with the specific catalytic effect of glucose oxidase, the present sensing strategy can be successfully expanded to detect glucose in blood. The preliminary results are in good agreement with those provided by the hospital, which suggests the generalizability and great potential of the Au NCs/Fenton hybrid system for research and clinical diagnosis of diabetes.

Received 6th February 2017  
Accepted 10th May 2017

DOI: 10.1039/c7ra01498h

rsc.li/rsc-advances

## 1. Introduction

Glucose, as a major energy source for living systems and metabolic intermediates, is closely associated with human health.<sup>1–4</sup> High levels of glucose in blood can lead to diabetes, a very common disease that seriously threatens the health of human beings. For effective management of diabetes and reduction of associated complications, frequent monitoring and tight control of blood glucose levels are highly required. To date, various approaches to glucose sensing in diabetes have been actively explored. Among these methods, the optical spectrum analysis of hydrogen peroxide ( $\text{H}_2\text{O}_2$ ) produced from glucose oxidase catalysis of glucose has proved to be a popular and effective way.<sup>5–10</sup> As one of the most reactive oxygen species,  $\text{H}_2\text{O}_2$  is not only associated with many physiological processes but also is an important mediator in food, pharmaceutical, clinical, industrial and environmental analyses.<sup>11–13</sup> Thus, the determination of hydrogen peroxide has also been an important task in the field of bio-imaging, healthcare and anti-terrorism. Continuing efforts in detecting  $\text{H}_2\text{O}_2$  have been focused on

different strategies including infrared/Raman spectroscopy, chromatography and electrochemical methods.<sup>14–16</sup> Although these methods made great contributions in  $\text{H}_2\text{O}_2$  and glucose detection, they often suffer from drawbacks, such as the requirement of expensive bulky equipment, long analysis time, complicate procedures and high detection limit. In this regard, it is still in great need of an inexpensive platform for reliable and rapid detection of  $\text{H}_2\text{O}_2$ .

$\text{H}_2\text{O}_2$ , with an electrochemical potential of 1.77V, can serve as an oxidizing agent. This property has been well studied and employed to control particle size and shape in the synthesis of nanomaterials.<sup>17–20</sup> Most importantly, the prominent oxidizing nature of  $\text{H}_2\text{O}_2$  has also been highlighted for successful development of effective  $\text{H}_2\text{O}_2$  sensors. For example, oxidation induced dissolution of silver/gold nanoparticles (Ag NPs/Au NPs) in the presence of  $\text{H}_2\text{O}_2$  has been demonstrated in several kinetic and mechanistic studies.<sup>21–24</sup> Notably, these oxidation processes often accompanied by a visible color and surface plasmon resonance (SPR) changes due to the unique size- and shape-dependent SPR properties of Ag NPs/Au NPs. Although these methods enable naked-eye detection of  $\text{H}_2\text{O}_2$ , the stabilization of Ag NPs/Au NPs is a challenging topic in practical application due to their easy oxidation (for Ag NPs) and aggregation. To address this issue, fluorescent quantum dots (QDs) have attracted wide attention.<sup>25–28</sup> Comparing with the colorimetric analysis, the QDs-based fluorescent detection method exhibits more advantages, such as high sensitivity and selectivity. However, the heavy metal

<sup>a</sup>Jiangsu Key Laboratory of Green Synthesis for Functional Materials, School of Chemistry and Material Science, Jiangsu Normal University, Xuzhou, Jiangsu 221116, China

<sup>b</sup>Department of Physical Sciences, Charleston Southern University, Charleston, South Carolina, USA. E-mail: yuyang@jsnu.edu.cn; Fax: +86-516-83536266

† Electronic supplementary information (ESI) available. See DOI: 10.1039/c7ra01498h

ion-containing QDs commonly suffer from intrinsic limitations, such as complicate modification, potential toxicity, intrinsic blinking and chemical instability.<sup>29,30</sup>

In order to avoid these disadvantages, we focused on gold-based nanoclusters (Au NCs). Compared to silver/gold nanoparticles and QDs, Au NCs, consisting of several to tens of gold atoms, have obvious superiority in sensing applications since they are non-toxic, high fluorescent, and have improved biocompatibility and stability. More importantly, the fluorescence of the Au NCs is highly sensitive toward sizes and changes of protecting agents.<sup>31,32</sup> To date, various types of H<sub>2</sub>O<sub>2</sub> sensors have been developed based on AuNCs. For example, Zhang has reported the first photoelectrochemical H<sub>2</sub>O<sub>2</sub> sensor based on mercaptoundecanoic acid protected Au NCs (MUA-Au NCs), but it suffers from some drawbacks including limited sensitivity and poor linearity.<sup>33</sup> Molaabasi has used haemoglobin capped Au NCs (Hb-Au NCs) for the detection of H<sub>2</sub>O<sub>2</sub> by taking advantages of the sensitive nature of Hb-Au NCs and the oxidizing property of H<sub>2</sub>O<sub>2</sub>.<sup>34</sup> This method offered an improved sensitivity and linearity, however, it needed long analysis time. Besides, the blue emission of the Hb-Au NCs may be interfered by the background autofluorescence of the serum samples. Recently, horseradish peroxidase (HRP) functioned fluorescent Au NCs that possess dual functions including catalysis ability and fluorescence have been designed for H<sub>2</sub>O<sub>2</sub> detection.<sup>35</sup> In this case, H<sub>2</sub>O<sub>2</sub> can be catalyzed by the HRP shell, leading to a significant quenching of the fluorescent gold core. This method offers a good sensitivity and fast response, but it pose a great challenge when using in complex system such as serum, since the activity of HRP can be easily affected. By combining the prominent sensitive nature of the Au NCs with Fenton reaction, we propose herein a rapid and effective strategy for H<sub>2</sub>O<sub>2</sub> and glucose detection. In the present case, Fe<sup>2+</sup> served as a catalyst to disproportionate H<sub>2</sub>O<sub>2</sub> to produce hydroxyl radical (<sup>•</sup>OH) through the so-called Fenton reaction.<sup>36–38</sup> The produced radical species are extremely reactive which can oxidize not only the thiol group of the protecting agent, but also the Au atoms in Au NCs. Therefore, sensitive detection of H<sub>2</sub>O<sub>2</sub> can be achieved. Moreover, since the oxidizing ability of the produced radical species is much stronger than H<sub>2</sub>O<sub>2</sub>, the response rate could thus be significantly improved.

Compared with the known optical H<sub>2</sub>O<sub>2</sub> detection strategies, our proposed method possesses some remarkable features. First, the Au NCs were fabricated with a simple, environment friendly method, thus minimizing cost and avoiding the use of toxic ions or organic reagents. Second, the fluorescence behavior of Au NCs are highly size- and surface protecting agent-dependent, hence making the present sensing strategy theoretically simple and low technical demands. In particular, the red emission of the Au NCs can decrease the interference from the background autofluorescence of the serum samples effectively. Third, the oxidizing ability of <sup>•</sup>OH produced from the Fenton reaction is much stronger than that of H<sub>2</sub>O<sub>2</sub>, and therefore affording a better sensitivity and fast response. Forth, only 100 to 200  $\mu$ L of serum could well meet the detection requirement owing to the high sensitivity. The whole processes could be accomplished within minutes. We believe such

simple and low-cost H<sub>2</sub>O<sub>2</sub> and glucose sensor has great potential in applications of point-of-care diagnostics.

## 2. Experimental

### 2.1 Reagents and apparatus

All reagents were of analytical grade and used without further purification. Ferrous sulfate (FeSO<sub>4</sub>·7H<sub>2</sub>O), HAuCl<sub>4</sub>·3H<sub>2</sub>O and glucose oxidase (EC 1.1.3.4) were bought from Sigma-Aldrich. Bull Serum Albumin (BSA), hydrogen peroxide (H<sub>2</sub>O<sub>2</sub>, 30 wt%), sodium hydroxide (NaOH), glucose, fructose, lactose, sucrose, maltose, mannose and other salts were purchased from Aladdin Chemical Company (Shanghai, China). Water was purified through a millipore system.

The fluorescence intensity spectra were recorded on an F-4600 fluorescence spectrometer (Hitachi Co., Japan). XPS was performed using a VGESCALAB MKII spectrometer. The XPSPEAK software was used to deconvolute the narrow-scan XPS spectra of the Au 4f of the Au NCs, using adventitious carbon to calibrate the C1S binding energy (284.5 eV). A PHS-3C pH (Shanghai Analytical Instrument Factory, Shanghai, China) meter was used to adjust pH values.

### 2.2 Fluorescence detection of H<sub>2</sub>O<sub>2</sub> and glucose

The BSA-stabilized Au NCs were synthesized according to a method described in a previous report.<sup>39</sup> Briefly, HAuCl<sub>4</sub> solution (5 mL, 10 mM) was added to BSA solution (5 mL, 50 mg mL<sup>-1</sup>) under vigorous stirring at 37 °C. Two minutes later, NaOH solution (0.5 mL, 1 M) was introduced and the reaction was allowed to proceed under vigorous stirring for 12 h at 37 °C. A typical H<sub>2</sub>O<sub>2</sub> detection procedure by using the as-prepared Au NCs was conducted as follows: 50  $\mu$ L of as-prepared Au NCs solution were diluted by 950  $\mu$ L water, and then HCl was added to adjust the pH value. 8  $\mu$ L Fe<sup>2+</sup> (40 mM) were then added as catalysis to induce the production of radical species. Subsequently, 2  $\mu$ L of H<sub>2</sub>O<sub>2</sub> solution with different concentrations was added to the above mixture and was incubated at room temperature for 8 min. Finally, the fluorescence emission spectra were collected.

For glucose detection, different concentrations of glucose (100  $\mu$ L) were mixed with 400  $\mu$ L of 0.5 mg mL<sup>-1</sup> GOx formulated with HAc-NaAc (pH 5.1) and incubated at 37 °C for an hour. Then 10  $\mu$ L of the mixture was added to the sensing system and incubate for 8 min. The fluorescence intensities were recorded in the wavelength range of 550–800 nm.

The selectivity of the sensing system toward glucose was evaluated by using sucrose, mannose, cellobiose, lactose, fructose, maltose, folic acid and typisin. Moreover, the selectivity of the sensing system toward common cations (*e.g.*, K<sup>+</sup>, Ca<sup>2+</sup>, Mg<sup>2+</sup>, Zn<sup>2+</sup> and Cu<sup>2+</sup>) was also evaluated by using their corresponding nitrates. In the case of Cu<sup>2+</sup>, polyethyleneimine (PEI, *M*<sub>w</sub> = 25 000) was used to chelate and separate Cu<sup>2+</sup>.

The procedure for glucose detection in serum was as follows: human serum samples were obtained from healthy volunteers treated in local hospital. The samples were centrifuged at 12 000 rpm for 10 min to remove the possible interference of



proteins in human serum. 100  $\mu\text{L}$  of serum samples and 400  $\mu\text{L}$  of 0.5  $\text{mg mL}^{-1}$  GOx were incubated at 37  $^{\circ}\text{C}$  for an hour. Then 10  $\mu\text{L}$  of the above mixture was added to the Au NCs sensing system as mentioned above and incubate for 8 min. Finally, the fluorescence intensity was collected at room temperature. All fluorescence detections were performed under the same conditions.

### 2.3 Live subject statement

The author state that the blood related experiments were performed in strict accordance with the WHO guidelines on blood drawing (WHO Publication ISBN-13: 978-92-4-159922-1, 2010) and was approved by Jiangsu Normal University. The authors also state that informed consent was obtained for any experimentation with human subjects and the Jiangsu Normal University is committed to the protection and safety of human subjects involved in research.

## 3. Results and discussion

### 3.1 Mechanism for fluorescence quenching of Au NCs

Bovine serum albumin (BSA) stabilized Au NCs were prepared according to a method described previously.<sup>39</sup> Transmission

electron microscopy (TEM) images reveal that the as-prepared Au NCs have an average diameter of *ca.* 1.2 nm (Fig. S1†). As shown in Fig. 1A, the initial solution of the as-prepared Au NCs exhibited a bright red fluorescence with the maximum emission spectra centered at 660 nm upon excitation at 529 nm. It is well known that  $\text{H}_2\text{O}_2$  can generate extremely oxidative hydroxyl radicals in the presence of  $\text{Fe}^{2+}$ , so called Fenton reaction, which has been widely applied in wastewater treatment.<sup>36</sup> Herein, we take advantage of Fenton reaction to accelerate fluorescence quenching of Au NCs in the presence of  $\text{H}_2\text{O}_2$  to sensitive and selective detect  $\text{H}_2\text{O}_2$  and glucose (Scheme 1). After 20  $\mu\text{M}$   $\text{H}_2\text{O}_2$  was added to the Au NCs- $\text{Fe}^{2+}$ -HCl system, the corresponding emission intensity of the sensing system was completely quenched (Fig. 1A). Notably, this quenching efficiency was much larger than that of  $\text{H}_2\text{O}_2$ . Dong *et al.* reported that 0.5 mM  $\text{H}_2\text{O}_2$  could induce 45% quenching of the fluorescence of Au NCs in 30 min.<sup>40</sup> Impressively, our experiments showed that 10  $\mu\text{M}$   $\text{H}_2\text{O}_2$  could reduce 76% of the fluorescence of Au NCs within 8 min. This increased quenching efficiency was reasonable considering the fact that the oxidizing ability of  $\cdot\text{OH}$  produced from Fenton reaction is much stronger than that of  $\text{H}_2\text{O}_2$ . Therefore,  $\cdot\text{OH}$  could lead to a more efficient

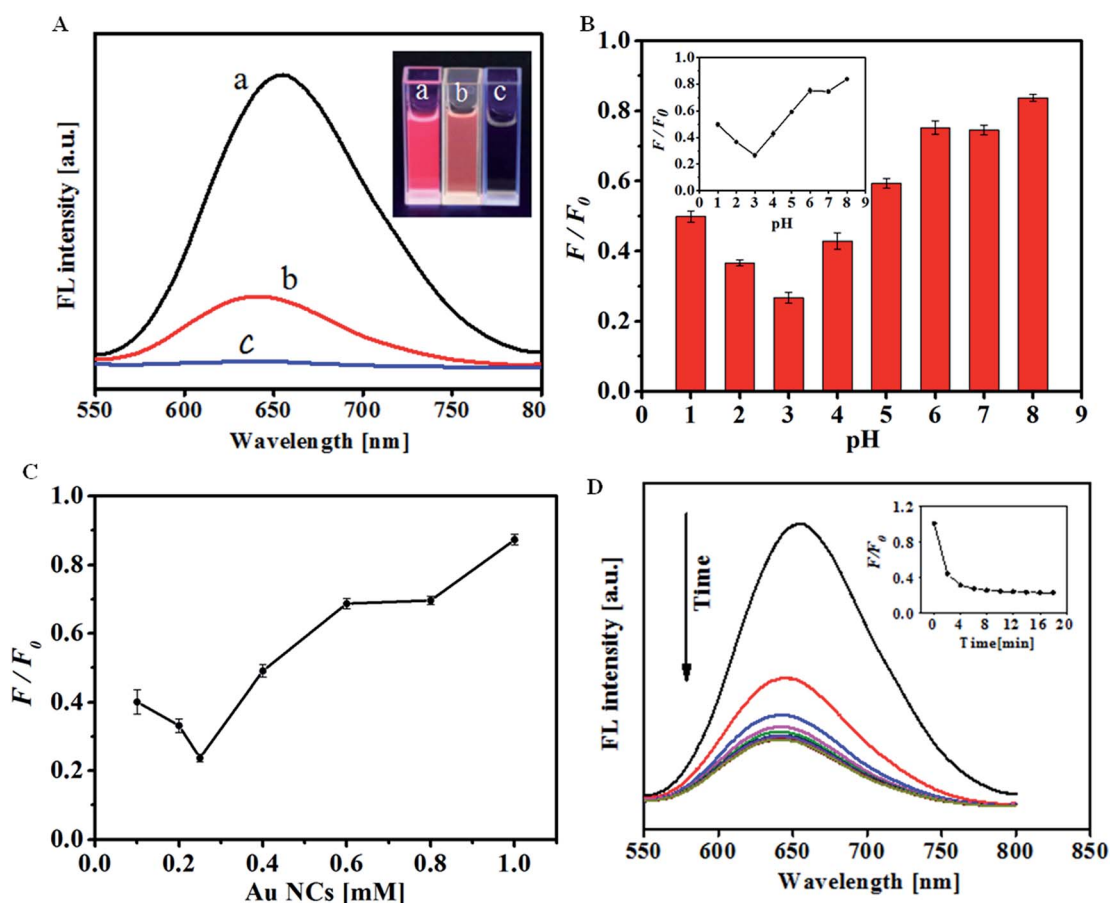
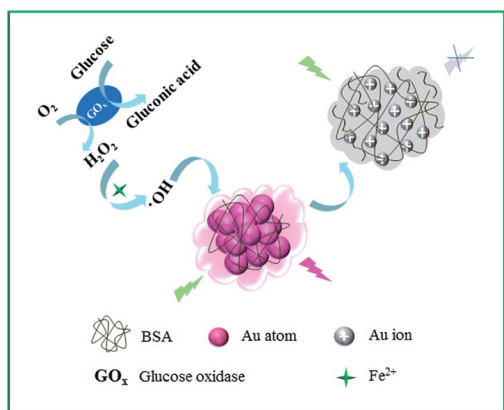


Fig. 1 (A) Fluorescence response of the Au NCs in the absence (a) and presence of 10  $\mu\text{M}$   $\text{H}_2\text{O}_2$  (b) and 20  $\mu\text{M}$   $\text{H}_2\text{O}_2$  (c) respectively; (B) fluorescence response of the Au NCs toward 10  $\mu\text{M}$   $\text{H}_2\text{O}_2$  at different pH values; (C) relationship between  $F/F_0$  and the concentration of Au NCs in the presence of 10  $\mu\text{M}$   $\text{H}_2\text{O}_2$ ; (D) time-dependent fluorescence response of the Au NCs to 10  $\mu\text{M}$   $\text{H}_2\text{O}_2$  ( $F_0$  and  $F$  are the fluorescence intensity of the  $\text{H}_2\text{O}_2$  at 660 nm in the absence and presence of  $\text{H}_2\text{O}_2$ , respectively).





**Scheme 1** Principle representation of the developed method for  $\text{H}_2\text{O}_2$  and glucose sensing.

quenching of the Au NCs and provide an improved sensitivity and oxidation rate. To understand the origin of the outstanding sensing performance of the present sensing system toward  $\text{H}_2\text{O}_2$ , possible interactions between Au NCs and  $\text{H}_2\text{O}_2$  in the presence of  $\text{Fe}^{2+}$  were further investigated by X-ray photoelectron spectroscopy (XPS) analysis. For the as-prepared Au NCs, the Au  $4f_{7/2}$  peak in the XPS spectrum at 83.7 eV is in good agreement with previous literature value.<sup>41</sup> Whereas, this peak shifted to a higher binding energy (84.7 eV) upon the addition of  $\text{H}_2\text{O}_2$  (Fig. S2†), which indicated the oxidation of the Au atoms in Au NCs.<sup>42</sup> Besides, previous studies have confirmed that Au-S bond can be degraded in the presence of  $\text{H}_2\text{O}_2$  as an oxidant to form disulfides and sulfonates which can be easily removed from the Au surface.<sup>40,43</sup> Considering the above facts and the stronger oxidizing ability of  $\cdot\text{OH}$ , it is reasonable to believe that oxidation of the Au-S bond may also occur during the  $\text{H}_2\text{O}_2$  recognition process. To verify this assumption, the absorption spectra of the Au NCs in the presence and absence of  $\text{H}_2\text{O}_2$  were recorded, respectively. As shown in Fig. S3,† the original Au NCs exhibited a characteristic absorbance at 278 nm, which mainly originates from the aromatic residues and disulfide bonds in BSA, the stabilizing protein in Au NCs.<sup>44</sup> However, this peak shifted distinctly in the presence of  $10\ \mu\text{M}$   $\text{H}_2\text{O}_2$ , which could be assigned to the oxidation of the composition of BSA as suggested by previous reports.<sup>40,45</sup> The above results clearly indicated that both the protecting BSA molecule and the Au atoms were oxidized during the course of  $\text{H}_2\text{O}_2$  response. Thus, it is reasonable to conclude that the effective fluorescence quenching of the sensing system in the presence of  $\text{H}_2\text{O}_2$  could ascribe to the oxidation-induced destruction of the Au NCs.

### 3.2 Optimization of the sensing parameters and detection of $\text{H}_2\text{O}_2$

It is known that the catalytic decomposition of  $\text{H}_2\text{O}_2$  by  $\text{Fe}^{2+}$  depends on the pH value of the reaction media. In order to achieve sensitive detection of  $\text{H}_2\text{O}_2$  and glucose, effect of the pH value on the fluorescence response of  $\text{H}_2\text{O}_2$  was studied and optimized. According to previous reports, the Fenton reaction is more favored in acidic medium<sup>36</sup> and thus, pH value higher than 8.0 was not considered. Fig. 1B shows the quenching

efficiency as a function of pH value. In the studied pH range of 1.0–8.0, the quenching efficiency of the sensing system in the presence of  $\text{H}_2\text{O}_2$  was gradually increased with increasing pH from 1 to 3, reached the maximum at pH 3.0, and then gradually decreased at higher pH (4–8). Based on the above results, pH 3.0 was chosen for further determination assays. Furthermore, the quenching efficiency of  $\text{H}_2\text{O}_2$  in the presence of  $\text{Fe}^{2+}$  as a function of the concentration of Au NCs was assessed. It was found that the fluorescence quenching is more efficient at lower concentration of the fluorescence probe (Fig. 1C) in the presence of a given concentration of  $\text{H}_2\text{O}_2$ . In the present case,  $0.25\ \text{mM}$  Au NCs was selected for the subsequent experiments. Moreover, to quantify the response rate of the sensing system, the time dependent fluorescence response of the sensing system to  $10\ \mu\text{M}$   $\text{H}_2\text{O}_2$  was monitored at 660 nm with an excitation wavelength of 529 nm (Fig. 1D). The curve shows a rapid decrease of the fluorescence intensity in the first 6 min, and kept almost unchanged after 8 min, which suggests that 8 min is enough for the detection of  $\text{H}_2\text{O}_2$ .

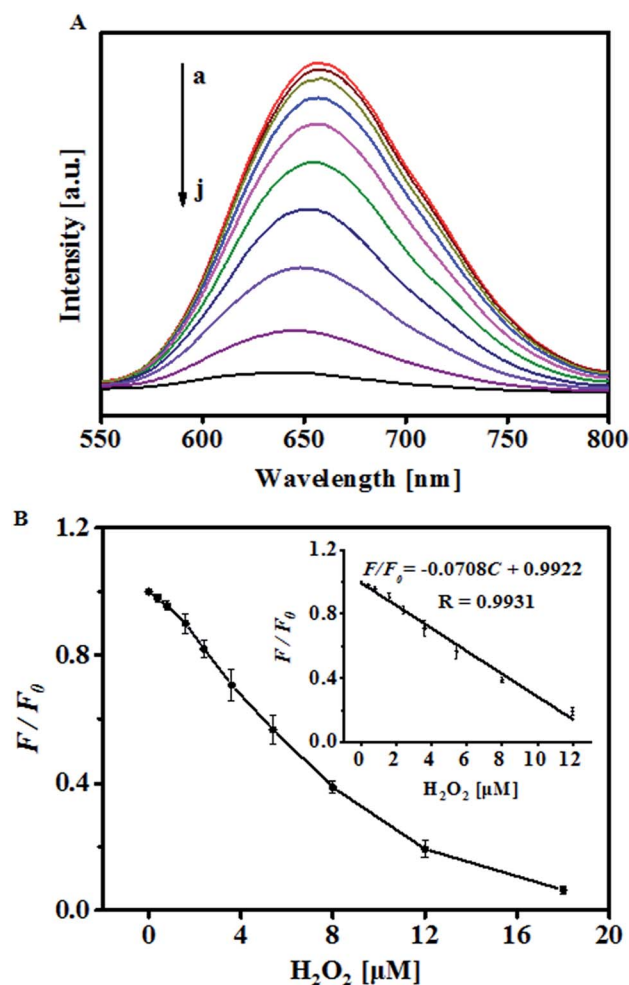


**Fig. 2** (A) Fluorescence response of the Au NCs upon addition of various concentrations of  $\text{H}_2\text{O}_2$  at a pH value of 3 ( $\text{H}_2\text{O}_2$  concentrations from a to j ( $\mu\text{M}$ ): 0; 0.4; 0.8; 1.6; 2.4; 3.6; 5.4; 8; 12 and 18); (B) the relationship between  $F/F_0$  and the concentration of  $\text{H}_2\text{O}_2$ . The inset is the linear plot in the range of 0 to  $12\ \mu\text{M}$   $\text{H}_2\text{O}_2$ .



Under the optimized conditions, the capability of the proposed strategy to sensitively and selectively detect  $\text{H}_2\text{O}_2$  was evaluated. Plotting  $F/F_0$  ( $F_0$  and  $F$  refer to the fluorescence intensity of the sensing system in the absence and presence of  $\text{H}_2\text{O}_2$ , respectively) as a function of  $\text{H}_2\text{O}_2$  concentration shows a good linear relationship over the concentration range from 0.4 to 12  $\mu\text{M}$ , which clearly validates the sensing performance of the proposed strategy toward  $\text{H}_2\text{O}_2$  (Fig. 2). The limit of the detection for  $\text{H}_2\text{O}_2$ , at a signal-to-noise ratio of 3, is 0.2  $\mu\text{M}$ , which is lower than some other optical methods (Table S1†). The percent relative standard deviation was 3.32% with five replicate detections of 10  $\mu\text{M}$   $\text{H}_2\text{O}_2$  (Table S2†), which indicated a good reproducibility of the present method.

### 3.3 Glucose sensing based on the Au NCs/Fenton and glucose oxidase system

Considering that GOx can catalyze the oxidation of glucose to produce  $\text{H}_2\text{O}_2$ , the successful sensitive detection of  $\text{H}_2\text{O}_2$  was, then, implemented for the analysis of glucose. The process for detecting glucose includes two steps: firstly,  $\text{H}_2\text{O}_2$  is generated from the biocatalyzed reaction between varied concentration of glucose and excess amount of GOx. Secondly, a certain volume of the resulted mixture was introduced into the sensing system for 8 min and then the corresponding fluorescence spectra were measured. Fig. 3 displays that the fluorescence intensity of Au NCs reduced gradually with increasing concentration of glucose. Controlled experiments showed that  $\text{O}_2$ , glucose oxidase, and glucose were all essential to the quenching of Au NCs (Fig. 3A inset) since the exclusion of either component would yield no  $\text{H}_2\text{O}_2$ . After optimizing the experimental parameters, a linear calibration curve is achieved by plotting  $F/F_0$  versus glucose concentration in the range of 2–60  $\mu\text{M}$  (Fig. 3B). A detection limit of 0.8  $\mu\text{M}$  was calculated from the equation (signal/noise = 3). To investigate whether this sensing system is specific for glucose detection, the effect of some other carbohydrates and metal ions

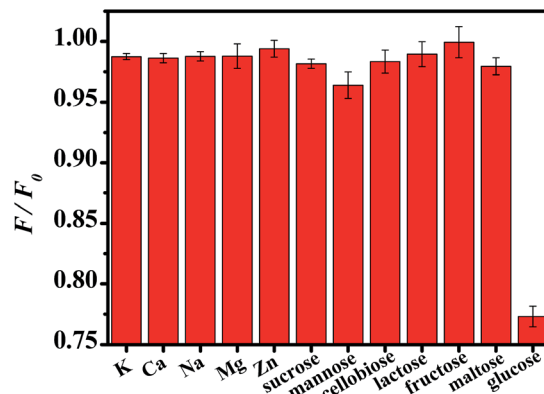


Fig. 4 The relative fluorescence intensity of the Au NCs in the presence of 10  $\mu\text{M}$  various carbohydrates and some metal ions commonly exist in serum.

that commonly present in human blood on the fluorescence of the sensing system were evaluated under the optimum conditions. As demonstrated in Fig. 4, the addition of glucose could induce a significant quenching of the Au NCs fluorescence due to the high substrate specificity of GOx. However, other carbohydrates and metal ions had a negligible effect under the identical conditions. Considering that trypsin, folic acid (FA) and  $\text{Cu}^{2+}$  were reported to quench the fluorescence of the Au NCs,<sup>46–49</sup> thus, the fluorescence response of our sensing system towards these substance were further examined. As shown in Fig. S4,† no obvious fluorescence change was observed even in the presence of high concentrations of trypsin and FA. This results is explainable since the low pH condition (pH = 3.0) selected in our system can not only weaken the interaction between FA and BSA *via* protonating both of them but also denature the trypsin. Also, it is noted that  $\text{Cu}^{2+}$  with high concentration do have an effect on the fluorescence intensity of the BSA-Au NCs as reported by Lin,<sup>48</sup> but such interference could be evaded by adding polyethyleneimine

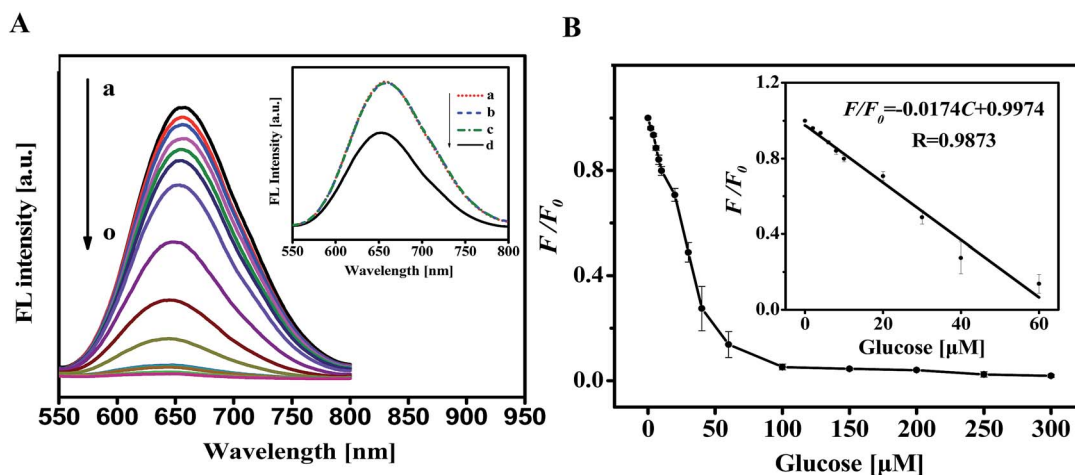


Fig. 3 (A) Fluorescence spectra represent the quenching effect of glucose–GOx system with different glucose concentrations on the fluorescence of Au NCs, glucose concentration from a to o ( $\mu\text{M}$ ): 0; 2; 4; 6; 8; 10; 20; 30; 40; 60; 100; 150; 200; 250; 300. Inset: fluorescence spectra of Au NCs (a); Au NCs with glucose oxidase (0.4  $\text{mg L}^{-1}$ ) (b); Au NCs with glucose (20  $\mu\text{M}$ ) (c); Au NCs with glucose (20  $\mu\text{M}$ ) and glucose oxidase (0.4  $\text{mg L}^{-1}$ ) (d); (B) the relationship between  $F/F_0$  and the concentration of glucose. The inset is the linear plot in the range of 0 to 60  $\mu\text{M}$  glucose.



Table 1 Analytical results of glucose in serum samples

| Sample no. | Local hospital (mM) | Proposed method (mM) | Relative deviation (%) |
|------------|---------------------|----------------------|------------------------|
| 1          | 4.59                | 4.65                 | 1.30                   |
| 2          | 4.96                | 4.86                 | −2.02                  |
| 3          | 5.25                | 5.34                 | 1.71                   |
| 4          | 12.59               | 12.12                | −3.73                  |
| 5          | 5.09                | 4.94                 | −2.95                  |

(PEI) as scavengers (Fig. S4c†). Therefore, sensitive and selective detection of glucose can be achieved through our proposed method. Moreover, comparable fluorescence response toward 10  $\mu\text{M}$   $\text{H}_2\text{O}_2$  were performed by using Au NCs stored at 4  $^\circ\text{C}$  for one and two weeks, respectively. The negligible change (the percent relative standard deviation is 2.76%) of the fluorescence response as presented in Table S3† indicated the good stability and reproducibility of our sensing system. Due to the above merits, the present method is expected to have a general applicability for detecting glucose in blood.

### 3.4 Determination of glucose in real serum samples

Glucose levels in blood are associated closely with diabetes or hypoglycemia. Thus it is of great importance to accurately monitor blood glucose levels for diagnosis and management of diabetes. Encouraged by the above promising results, the sensing system was further applied to monitor glucose in real serum samples. In this case, the fresh human serum samples were obtained from a local hospital and used as testing samples after simple centrifugation treatment. Taking into consideration of the normal fasting blood glucose (FBG) level in the healthy human blood (3.9–6.1  $\text{mmol L}^{-1}$ ) as well as the linear range of our method, 100  $\mu\text{L}$  of serum should well meet one-time glucose measurement. In a proof of concept experiment, 100  $\mu\text{L}$  of the testing samples were firstly incubated with 400  $\mu\text{L}$  GOx (0.5  $\text{mg mL}^{-1}$ ) for an hour, then 10  $\mu\text{L}$  of the resulted mixture was added to the sensing system (1 mL) and the fluorescence spectra were measured. It is worthy to note that the serum samples were 500-fold diluted during the process and therefore, the possible interference from the serum matrix could be significantly reduced. The concentrations of the clinical samples were calculated from the standard curve and the regression equation. Impressively, the glucose concentration obtained by our method is in good agreement with those provided by the hospital (Table 1), which further confirms the general applicability of the proposed method for the analysis of glucose in real physiological clinical samples.

## 4. Conclusion

By combining the Fenton reaction with the prominent sensitive nature of the Au NCs, a rapid, highly sensitive, selective, and cost-efficient sensing approach for  $\text{H}_2\text{O}_2$  and glucose detection has been designed. The sensing approach was successfully applied to monitor glucose levels in human serum with

satisfactory results. The sensing strategy proposed in this study is very promising in pharmaceutical and clinical detection of  $\text{H}_2\text{O}_2$  and glucose due to the advantages of easy fabrication and operation. We anticipate that the designed strategy can also be extended to the detection of various  $\text{H}_2\text{O}_2$ -involved analytes. This may open up a new avenue in developing low-cost and sensitive method for biological and clinical diagnostics application.

## Acknowledgements

The authors would like to acknowledge the financial support from the Natural Science Foundation of China (NSFC 21601072), Natural Science Foundation of Jiangsu Province (BK20150228), Natural Science Foundation of the Higher Education Institutions of Jiangsu Province (16KJA150006) and Priority Academic Program Development of Jiangsu Higher Education Institutions.

## References

- 1 M. A. Pleitez, T. Lieblein, A. Bauer, O. Hertzberg, H. von Lilienfeld-Toal and W. Mantele, *Anal. Chem.*, 2013, **85**, 1013–1020.
- 2 Y. Ling, N. Zhang, F. Qu, T. Wen, Z. F. Gao, N. B. Li and H. Q. Luo, *Spectrochim. Acta, Part A*, 2014, **118**, 315–320.
- 3 Y. Yi, J. Deng, Y. Zhang, H. Li and S. Yao, *Chem. Commun.*, 2013, **49**, 612–614.
- 4 H. B. Wang, H. D. Zhang, Y. Chen, Y. Li and T. Gan, *RSC Adv.*, 2015, **5**, 77906–77912.
- 5 L. Wang, J. Zheng, Y. Li, S. Yang, C. Liu, Y. Xiao, J. Li, Z. Cao and R. Yang, *Anal. Chem.*, 2014, **86**, 12348–12354.
- 6 O. S. Wolfbeis, A. Durkop, M. Wu and Z. H. Lin, *Angew. Chem., Int. Ed.*, 2002, **41**, 4495–4498.
- 7 S. Chen, X. Hai, X. W. Chen and J. H. Wang, *Anal. Chem.*, 2014, **86**, 6689–6694.
- 8 L. P. Lin, X. H. Song, Y. Y. Chen, M. C. Rong, T. T. Zhao, Y. R. Wang, Y. Q. Jiang and X. Chen, *Anal. Chim. Acta*, 2015, **869**, 89–95.
- 9 L. Z. Hu, Y. L. Yuan, L. Zhang, J. M. Zhao, S. Majeed and G. B. Xu, *Anal. Chim. Acta*, 2013, **762**, 83–86.
- 10 H. B. Wang, Y. Chen, N. Li and Y. M. Liu, *Microchim. Acta*, 2017, **184**, 515–523.
- 11 D. J. Rossi, C. H. M. Jamieson and I. L. Weissman, *Cell*, 2008, **132**, 681–696.
- 12 N. E. Sharpless and R. A. Depinho, *Nat. Rev. Mol. Cell Biol.*, 2007, **8**, 703–713.
- 13 D. Srikun, A. E. Albers, C. I. Nam, A. T. Iavarone and C. J. Chang, *J. Am. Chem. Soc.*, 2010, **132**, 4455–4465.
- 14 W. Chen, S. Cai, Q.-Q. Ren, W. Wen and Y.-D. Zhao, *Analyst*, 2012, **137**, 49–58.
- 15 T. H. Huang, M. E. Garceau and P. Gao, *J. Pharm. Biomed. Anal.*, 2003, **31**, 1203–1210.
- 16 L. L. Qu, Y. Y. Liu, S. H. He, J. Q. Chen, Y. Liang and H. T. Li, *Biosens. Bioelectron.*, 2016, **77**, 292–298.
- 17 W. Ni, X. Kou, Z. Yang and J. Wang, *ACS Nano*, 2008, **2**, 677–686.



- 18 M. Tsuji, S. Gomi, Y. Maeda, M. Matsunaga, S. Hikino, K. Uto, T. Tsuji and H. Kawazumi, *Langmuir*, 2012, **28**, 8845–8861.
- 19 Q. Zhang, C. M. Cobley, J. Zeng, L. P. Wen, J. Y. Chen and Y. N. Xia, *J. Phys. Chem. C*, 2010, **114**, 6396–6400.
- 20 Q. Zhang, N. Li, J. Goebel, Z. Lu and Y. Yin, *J. Am. Chem. Soc.*, 2011, **133**, 18931–18939.
- 21 K. Nitinaivinij, T. Parnklang, C. Thammacharoen, S. Ekgasit and K. Wongravee, *Anal. Methods*, 2014, **6**, 9816–9824.
- 22 Y. Xia, J. Ye, K. Tan, J. Wang and G. Yang, *Anal. Chem.*, 2013, **85**, 6241–6247.
- 23 X. M. Ma, Z. T. Chen, P. Kannan, Z. Y. Lin, B. Qiu and L. H. Guo, *Anal. Chem.*, 2016, **88**, 3227–3234.
- 24 G. Y. Shan, S. J. Zheng, S. P. Chen, Y. W. Chen and Y. C. Liu, *Colloids Surf., B*, 2013, **102**, 327–330.
- 25 R. Gill, L. Bahshi, R. Freeman and I. Willner, *Angew. Chem., Int. Ed.*, 2008, **47**, 1676–1679.
- 26 L. H. Cao, J. Ye, L. L. Tong and B. Tang, *Chem.–Eur. J.*, 2008, **14**, 9633–9640.
- 27 M. Hu, J. Tian, H. T. Lu, L. X. Weng and L. H. Wang, *Talanta*, 2010, **82**, 997–1002.
- 28 J. J. Ge, X. L. Ren, X. Z. Qiu, H. T. Shi, X. W. Meng and F. Q. Tang, *J. Mater. Chem. B*, 2015, **3**, 6385–6390.
- 29 A. M. Derfus, W. C. W. Chan and S. N. Bhatia, *Nano Lett.*, 2004, **4**, 11–18.
- 30 S. F. Lee and M. A. Osborne, *J. Am. Chem. Soc.*, 2007, **129**, 8936–8937.
- 31 P. C. Chen, A. P. Periasamy, S. G. Harroun, W. P. Wu and H. T. Chang, *Coord. Chem. Rev.*, 2016, **320**, 129–138.
- 32 L. Y. Chen, C. W. Wang, Z. Q. Yuan and H. T. Chang, *Anal. Chem.*, 2015, **87**, 216–229.
- 33 J. Zhang, L. Tu, S. Zhao, G. Liu, Y. Wang, Y. Wang and Z. Yue, *Biosens. Bioelectron.*, 2015, **67**, 296–302.
- 34 F. Molaabasi, S. Hosseinkhani, A. A. Moosavi-Movahedi and M. Shamsipu, *RSC Adv.*, 2015, **5**, 33123–33135.
- 35 F. Wen, Y. Dong, L. Feng, S. Wang, S. Zhang and X. Zhang, *Anal. Chem.*, 2011, **83**, 1193–1196.
- 36 E. F. Olasehinde, S. Makino, H. Kondo, K. Takeda and H. Sakugawa, *Anal. Chim. Acta*, 2008, **627**, 270–276.
- 37 H. H. Deng, G. W. Wu, D. He, H. P. Peng, A. L. Liu, X. H. Xia and W. Chen, *Analyst*, 2015, **140**, 7650–7656.
- 38 L. Zhang, R. P. Liang, S. J. Xiao, J. M. Bai, L. L. Zheng, L. Zhan, X. J. Zhao, J. D. Qiu and C. Z. Huang, *Talanta*, 2014, **118**, 339–347.
- 39 J. P. Xie, Y. G. Zheng and J. Y. Ying, *J. Am. Chem. Soc.*, 2009, **131**, 888–890.
- 40 L. H. Jin, L. Shang, S. J. Guo, Y. X. Fang, D. Wen, L. Wang, J. Y. Yin and S. J. Dong, *Biosens. Bioelectron.*, 2011, **26**, 1965–1969.
- 41 M. Brust, M. Walker, D. Bethell, D. J. Schiffrin and R. Whyman, *J. Chem. Soc., Chem. Commun.*, 1994, 801–802, DOI: 10.1039/c39940000801.
- 42 M. Dasog and R. W. J. Scott, *Langmuir*, 2007, **23**, 3381–3387.
- 43 C. Vericat, M. E. Vela, G. Benitez, P. Carro and R. C. Salvarezza, *Chem. Soc. Rev.*, 2010, **39**, 1805–1834.
- 44 L. Shang, Y. Z. Wang, J. G. Jiang and S. J. Dong, *Langmuir*, 2007, **23**, 2714–2721.
- 45 D. Y. Luo, S. W. Smith and B. D. Anderson, *J. Pharm. Sci.*, 2005, **94**, 304–316.
- 46 B. Hemmateenejad, F. Shakerizadeh-shirazi and F. Samari, *Sens. Actuators, B*, 2014, **199**, 42–46.
- 47 L. Hu, S. Han, S. Parveen, Y. Yuan, L. Zhang and G. Xu, *Biosens. Bioelectron.*, 2012, **32**, 297–299.
- 48 Z. Lin, F. Luo, T. Dong, L. Zheng, Y. Wang, Y. Chi and G. Chen, *Analyst*, 2012, **137**, 2394–2399.
- 49 Y. Tao, Y. Lin, J. Ren and X. Qu, *Biosens. Bioelectron.*, 2013, **42**, 41–46.

